
Article:
Bunce, A., Brennan, D.S., Ferguson, A. et al. (2024) On population-based structural health monitoring for bridges: comparing similarity metrics and dynamic responses between sets of bridges. Mechanical Systems and Signal Processing, 216. 111501. ISSN: 0888-3270

https://doi.org/10.1016/j.ymssp.2024.111501

Mechanical Systems and Signal Processing 216 (2024) 111501

Contents lists available at ScienceDirect

Mechanical Systems and Signal Processing

journal homepage: www.elsevier.com/locate/ymssp

On population-based structural health monitoring for bridges: Comparing similarity metrics and dynamic responses between sets of bridges

Andrew Bunce [a,*], Daniel S. Brennan [b], Alan Ferguson [a], Connor O'Higgins [a], Su Taylor [a], Elizabeth J Cross [b], Keith Worden [b], James Brownjohn [c], David Hester [a,*]

[a] Civil and Structural Engineering, School of Natural and Built Environment, Queens University Belfast, Stranmillis Road, Belfast BT7 1NN, United Kingdom
[b] Dynamics Research Group, University of Sheffield, Department of Mechanical Engineering, Mappin Street, Sheffield S1 3JD, United Kingdom
[c] Vibration Engineering Section, University of Exeter, Exeter Science Park, Clyst Honiton, Exeter EX5 2FN, United Kingdom

A B S T R A C T

Bridges are valuable infrastructure assets that are challenging and expensive to maintain. State-of-the-art data-based bridge SHM solutions look to use bridge response data for condition assessment and damage detection. Data-based SHM methods can be limited in their application as they require large datasets to train models effectively, and most bridges lack the available data for the approaches to work. Further, it would be expensive and unrealistic to collect the required datasets to employ data-based methods to entire bridge networks. Recently, a population-based structural health monitoring (PBSHM) approach was proposed that seeks to leverage the data available for SHM problems by pooling together similar structures with their datasets. The PBSHM approach could be valuable in bridge SHM, enhancing the datasets available for 'populations of bridges. The PBSHM approach for assessing the similarity of bridges has been considered before and was shown to be useful for identifying similar and different bridge types. However, no data were considered in the previous work, and similarity metrics were only qualified using engineering judgement. For the PBSHM approach to be useful in bridge SHM, there is still a need to check that 'similar' bridges have similar responses for transfer learning to be feasible. This paper expands upon previous work and provides originality by investigating if bridges identified as similar also exhibit similar responses. The PBSHM derived similarity metrics convey the topological similarity between structures, and mode shapes are identified as being a topologically sensitive bridge response. Therefore, a modal test campaign is carried out for a set of six real bridges, and Operational Modal Analysis is used to identify modal responses from each of the bridge decks. The Modal Assurance Criterion is used to evaluate the similarity between the mode shapes from pairs of bridges and is subsequently compared to the similarity metrics evaluated between those bridges. The similarity metrics were found to be reflective of the similarities identified between the respective bridges' mode shapes for bridges of the same and different types. The significance of this finding is that it is an important step towards validating the PBSHM comparison approach for identify similar structures where transfer learning might be attempted.

1. Introduction

The focus of this paper is on the application of population-based structural health monitoring (PBSHM) to bridges. For context, Section 1.1 provides a background on the topic of population-based structural health monitoring (PBSHM) and Section 1.2 details the PBSHM work towards systematically comparing structures for similarity. Section 1.3 presents the PBSHM work towards bridge applications, identifying the limitations of the work to date. Section 1.4 describes the contributions of this work, and how it specifically

* Corresponding authors.
E-mail addresses: abunce01@qub.ac.uk (A. Bunce), d.hester@qub.ac.uk (D. Hester).

https://doi.org/10.1016/j.ymssp.2024.111501
Received 4 January 2024; Received in revised form 13 April 2024; Accepted 3 May 2024
Available online 9 May 2024

addresses the identified limitations of PBSHM as applied to bridges.

1.1. Challenges in bridge SHM

Bridges are valuable infrastructure assets that have proven challenging to maintain. Traditional bridge management systems are strained, relying on visual inspections where an engineer would physically attend and inspect each element of a bridge, assigning a condition rating that is used to inform of bridge maintenance decisions [1]. Bridge SHM, i.e., the use of data in the assessment of a bridge, has been demonstrated to enhance bridge condition assessments [2]. State of the art bridge SHM approaches tend to be data based, where a data model is trained using real bridge data, and subsequent bridge response data is then compared. Variance between the bridge and data-model responses can be indicative of change in the bridge conditions. In recent years, there has been an emerging trend in data-based bridge SHM research that has implemented machine learning algorithms (MLAs) to exploit bridge response datasets [3]. However, many bridges have little history of data collection, if any history of data collection at all, therefore there are still challenges associated with the application of machine learning to bridge SHM.

Population-based structural health monitoring (PBSHM) is a relatively new approach that seeks to facilitate information sharing between structures. In principle, the approach posits that if two structures are similar enough, then there is scope to learn between the two structures. If a PBSHM approach could be implemented to bridges, there could be scope to enhance the tools available for bridge management. In broad terms, it would provide a platform for bridges to be managed and monitored as groups of structures, as opposed to being monitored in isolation as is the current standard. Pooling similar bridges together, with their associated datasets, means the collective data available for the SHM of each bridge would be more robust than any of the individual datasets that contributed to the pool. Even bridges with no history of data collection at all (including newly constructed bridges) could avail of historical benchmark data learnt from a pool of similar bridges, enabling the use of MLAs which otherwise, would be unavailable.

1.2. Population-Based structural health monitoring

Population-based structural health monitoring was first considered for wind farms as there is generally little variation among the set of turbines comprising a typical wind farm [4,5]. An early application of a PBSHM approach was demonstrated by Dervilis et al [6], where a neural network regression technique was implemented for the performance monitoring of a wind farm. The performance of each turbine was monitored relative to neighbouring turbines from the same wind farm, enhancing benchmark data available for anomaly detection. The performance of a similar neural network approach was compared with a Gaussian process regression (GPR) approach by Papatheou et al [7], where both anomaly-detection methods presented good damage-detection performance using the same power-curve response data from the wind farm (from wind speed vs power generated).

Wind farms are an example of a homogeneous population of structures. That is, variations between wind turbine structures in a typical wind farm are limited to manufacturing tolerances. Therefore, the entirety of a homogeneous population can be idealised by a single model, referred to as the 'Form' [8]. With a Form identified for a homogeneous population of structures, a single data model can then be trained for the SHM of that population [9]. General Form models trained from homogeneous population data have the distinct advantage of representing the in-situ behaviour of the population, rather than idealised healthy behaviour prediction [10]. In recent applications of PBSHM to wind turbines, a Gaussian process regression model was implemented for the PBSHM of a wind farm where environmental and operational variations (EOVs) were mapped across the wind farm [11]. Subsequently, a damage-mapping approach was trialled on the same wind farm, with the use of EOV information enhancing the performance of the anomaly detection system [12]. The PBSHM applications were made possible by the level of homogeneity amongst wind turbines in wind farms, and the consistency of available data. However, there are distinct challenges when considering a PBSHM application to heterogeneous populations of structures (i.e., structures that are nominally different), particularly with the risk of negative transfer [13].

Negative transfer refers to inferences being made that could reduce the performance of a monitoring system [14]. For example, negative transfer between bridges could lead to incorrect benchmarks being established for the SHM of those bridges which could result in either false triggers or damages going undetected. To limit the risk of negative transfer occurring between heterogeneous populations, the PBSHM approach has been explored in two main themes; (1) identifying structures that are similar, and (2) investigating what, if any, information may be sharable between those structures [15]. Irreducible Element models are the proposed method for capturing information about a structure. Attributed Graphs (AGs) are then generated from IE models, which allows graphs of structures to be compared using graph comparison techniques. Applications of PBSHM to heterogeneous populations have been limited to numerical models [16], or subsections of structures, such as aircraft wings [17], tailplanes [18] and helicopter blades [19]. Similarly, in the bridge SHM literature, transfer learning has only been used to transfer knowledge between real bridges and numerical models of those bridges [20], or between known identical pairs of elements [21,22]. For transfer learning to be feasible between disparate populations of real bridges, there is first a need to identify bridges that are similar enough for some level of knowledge to be transferrable.

1.3. Towards PBSHM for bridges

In the conception of PBSHM, and the development of IE models and AGs to compare structures for similarity, bridges have previously been represented with simplified "toy" structures [23,24]. The first application of the IE model schema and AG comparison tools to a set of real bridges resulted in the largest IE models and AGs of structures to date [25]. Five bridges of five distinct types were modelled and compared to ensure that the IE model schema was suitable for describing a range of bridge constructions and the AG

comparisons could be used to identify the differences between their topologies. Subsequently, three additional bridges were introduced to the set where the similarity metrics between bridges of the same type were much higher than between bridges of different types. Whilst positive, the resulting similarity metrics lacked significance, where one would not know which portions of bridges were similar without interrogating the maximum common subgraphs.

The PBSHM work has since developed problem-driven IE models that essentially describe subsections of existing whole-structure IE models [26]. The extents of the problem-driven IE model are set to mimic the extents of information being considered in the PBSHM/transfer learning problem. Subtle variations between graphs have a much greater impact on the resulting similarity metrics, enhancing the resolution of the AG comparisons. Whilst it has been shown that the similarity of structures may relate to similarity of feature states [27], it remains to be seen if bridges identified as similar have similar responses, and if bridges identified as different have different responses. The applications of the IE-model schema and AG comparison toolsets have been largely positive for bridge applications, though the results have only been qualified using engineering judgement to date.

1.4. Contributions of this paper

The work in this paper explores the next logical step in implementing a PBSHM approach to bridges; that is, it investigates if bridges identified as similar exhibit similar structural behaviour (i.e., response to operational loads), and if bridges identified as different exhibit different structural behaviour. As the PBSHM comparison approach focuses on topological similarity between bridges, this paper seeks to compare topologically sensitive data responses between bridges. Mode shapes are largely governed by structural form, and dynamic response data is typically easier to collect than other data types. Furthermore, the PBSHM work to data has shown that there is inferable SHM information contained within dynamic response data. [17,18,19].

Therefore, this paper demonstrates the IE modelling and AG comparison approach applied to a set of six real bridges of two distinct types and proposes a data-collection campaign to identify the modal responses from the set of bridges. The Modal Assurance Criterion (MAC) presents a measure of similarity between a pair of mode shapes and is therefore used to evaluate the similarity of the mode shapes between the set of bridges. This paper aims to check that the PBSHM comparison tools can be used to identify and pool together similar bridges that also have similar responses, such that there would be a high chance of successful knowledge transfer between the set of similar bridges. As bridges tend to be large and complex structures, only bridge decks are considered in this paper. The work in this paper presents a significant step towards the validation of PBSHM as a potentially useful tool in bridge SHM. In particular, the specific contributions of the paper are:

- IE models and AGs are used to describe and compare a set of six real bridge decks, and then a series of ambient vibration mode tests are carried out on that set of bridge decks.
- The modal responses from each of the six bridges are identified and subsequently compared using the Modal Assurance Criterion as a similarity metric, demonstrating that similar bridges have similar modal responses, and different bridges have different modal responses.
- Similarity metrics between the set of bridge decks (using the PBSHM comparison tools) are shown to reflect the similarity between the modal responses of those bridge decks.

The population of bridges used in this study is described in Section 2. Section 3 describes the IE models for the bridges and presents the similarity metrics from the AG comparisons between the set of bridges. Section 4 describes the modal tests carried out for each of the bridges and presents the MPs identified for each bridge. Section 5 provides a discussion on the calculated similarity metrics, considering the Modal Assurance Criterion values evaluated between the bridge mode shapes, and Section 6 presents the conclusions of the work.

Fig. 1. Truss 1: (a) elevation of truss footbridge, (b) bridge deck.

2. Population of bridges in this study

This section describes the bridges used in this paper. There were six bridges selected in total, of two distinct types:

- Two truss footbridges, described in Section 2.1.
- Four beam and slab highway bridges, described in Section 2.2.

2.1. Truss footbridges

The two truss footbridges used for this study (Truss 1 and Truss 2) were selected as they are two near-identical steel Warren type through truss footbridges of similar age. Fig. 1(a) shows the elevation of Truss 1, and (b) shows the deck of the bridge.

The footbridges have the same 2.5 m width and are supported on identical bearing systems atop similar support structures, with ancillary approach ramps and stairs. The main variation between the two bridge spans is the span length; however, with that comes more subtle variations in the bridge design, such as radius of the hollow sections that form the top and bottom chords, as well as length and relative angle of the inclined bracing members which affect bracing stiffness. Fig. 2 shows an elevation representing the two truss footbridges with the support structures greyed out. Table 1 provides summary information for the two truss footbridges.

2.2. Beam and slab highway bridges

The four beam and slab bridges used in this study (B&S1 – B&S4) were selected as they are a set of similar two-span integral-abutment highway bridges. Fig. 3(a) shows the bridge elevation for B&S1, and (b) shows the bridge deck viewed from the footpath at the abutment.

Each of the four beam and slab bridges in this paper are two-span integral abutment bridges. The bridge decks are cast *in situ* atop precast concrete beams, which are fixed in place atop the supports with concrete diaphragms.

Two beam and slab bridges (B&S1 and B&S2) are similar widths and are made up of four precast beams per span. The main variation between these two bridges is the span lengths (Table 2). B&S3 is longer and wider than B&S1 and B&S2 and comprises five precast beams per span. B&S4 is the longest and widest of the beam and slab bridges in this paper and has six precast beams per span.

Fig. 4(a) shows elevations of the beam and slab bridges (with support structures greyed out). Fig. 4 (b) shows cross-sections for B&S1 and B&S2. Fig. 4(c) and (d) show cross-sections for B&S3 and B&S4, respectively. Table 2 presents the summary information for each beam and slab bridge, including the span lengths, bridge widths and number of precast beams.

3. Comparing bridges for similarity

This section provides an overview of the irreducible element (IE) model and Attributed Graph (AG) comparison approach used in this paper. IE models are used to capture information about a structure that would be significant to that structure's response. AGs are generated from IE models, and facilitate comparisons between structures using graph comparison techniques [28,29].

The approach in this paper is largely similar to that used in [25], which involved modelling whole bridges to check that they *could* be compared for similarity using the PBSHM tools. However, this paper aims to compare the responses from a set of bridge decks, therefore, only the bridge deck structures are compared for similarity. To achieve this, problem-driven IE models are used to describe the bridge decks, where a problem driven IE model is effectively a subsection from a whole-structure IE model. Section 3.1 demonstrates the approach of describing a Truss footbridge deck with a problem driven IE model, and Section 3.2 demonstrates the approach of describing a Beam and Slab bridge deck with a problem driven IE model. Section 3.3 provides a demonstration of how a pair of AGs can be compared for similarity, offering context for the resulting similarity metrics that are evaluated, and Section 3.4 presents the similarity metrics from comparing all six bridges.

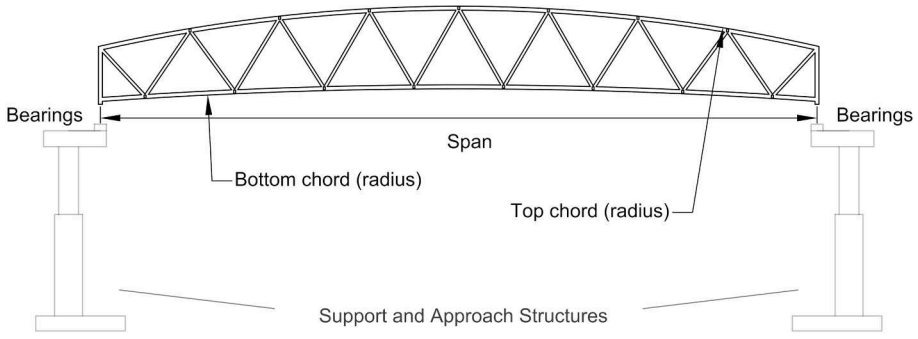

Fig. 2. Diagram of truss footbridge elevation.

Table 1
Truss footbridge summary information.

Bridge	Bottom chord radius	Top chord radius	Span
1 – Truss 1	360.4 *m*	112.5 *m*	36 *m*
2 – Truss 2	340.4 *m*	102.1 *m*	34 *m*

Fig. 3. B&S1: (a) elevation of beam and slab bridge, (b) bridge deck.

Table 2
Beam and slab bridge summary information.

Bridge	Width	# Beams	Beam Spacing	Span 1	Span 2	Total Span
3 – B&S1	12.8 *m*	4	3.05 *m*	28.0 *m*	26.0 *m*	54.0 *m*
4 – B&S2	13.2 *m*	4	3.1 *m*	29.5 *m*	28.0 *m*	57.5 *m*
5 – B&S3	16.4 *m*	5	3.1 *m*	29.0 *m*	32.0 *m*	61.0 *m*
6 – B&S4	17 *m*	6	2.7 *m*	35.0 *m*	29.5 *m*	64.5 *m*

3.1. Truss footbridges

To go from a real structure to a problem driven IE model, the first stage is to define the extents of the structure that the problem relates to and identify the constituent elements that make up that part of the structure. For the truss footbridges, the extents of the bridge deck were assumed to be at the bearing locations at each support. In a problem driven IE model, ground elements identify a third-party structure. In this instance, the ground elements detail the adjoining support structures, including approach ramps and stairs. The bearing locations annotated in Fig. 2 show the assumed ground elements of the bridge deck to be modelled, which would also reflect the extents of the bridge deck response data being considered (i.e., mode shapes).

The next stage is to identify the constituent elements that comprise the part of the structure to be modelled. For each element, the element's contextual type, coordinates, geometry, and material information are recorded. As this can be a subjective exercise, an IE model schema has been created that includes nomenclature to unify element and joint descriptions, limiting the influence of subjectivity in the IE modelling of structures [29]. For each of the bridges in this paper, construction drawings were used to identify the elements and their associated attributes for the IE models. The truss bridges were modelled to a high granularity, meaning that each element of the bridge was individually defined resulting a total of 149 regular elements between the two ground elements.

The final stage of the IE modelling process is to map the interactions (termed '*relationships*' in the IE models) between the elements of the bridge. Each relationship between pairs of elements is recorded with information about its type. For the truss footbridges, there were 295 relationships defined in each IE model.

The IE models in this paper were stored as Python scripts. Fig. 5 provides a sample of the first truss footbridge IE model (Truss 1). Fig. 5 (a) shows a sample '*ground*' element and '*regular*' element, and Fig. 5(b) shows a sample '*boundary*' relationship and '*static joint*' relationship.

3.2. Beam and slab bridges

The beam and slab bridges were modelled to the same procedure as the truss footbridges. However, the beam and slab bridges are two-span with an intermediate support and the main beams are cast integrally with diaphragms at each end. Therefore, the ground locations identified in the IE models were at the two abutments and intermediate support, where the boundaries were identified as being at the diaphragm – bearing interface and expansion joint locations. The information about the support structures (i.e., specific element information) was reduced to the ground elements of the models. Owing to a simpler construction type, the beam and slab

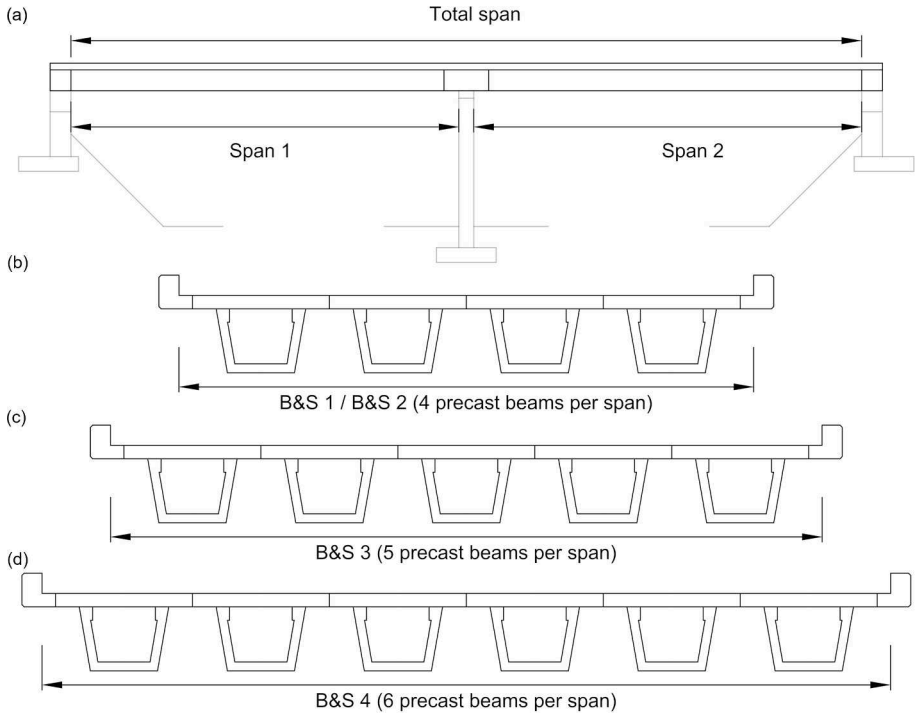

Fig. 4. Beam and slab bridge(s): (a) elevation applicable to B&S1 – B&S4, (b) cross-section of B&S1 and B&S2 bridge deck, (c) cross-section of B&S3 bridge deck, (d) cross-section of B&S4 bridge deck.

bridge deck IE models were significantly smaller than the truss footbridge deck IE models.

- The IE models for B&S1 and B&S2 comprised 28 elements, with 43 relationships.
- The IE model for B&S3 comprised 33 elements with 52 relationships, and
- The IE model for B&S4 comprised 38 elements with 61 relationships.

Once the IE models were created, they were each ingested to a custom Mongo DB database, where inbuilt functions (scripts) allowed for the generation and comparison of AGs [30].

3.3. Attributed graph comparisons

Attributed Graphs (AGs) are simply graph representations of IE models. No information is gained or lost when creating AGs from IE models; the information is simply converted such that nodes on the graph represent elements, and the vertices represent the interactions between elements. The primary reason for using AGs to represent structures is to facilitate the use of graph comparison tools to compare structures [31,32,33,34]. The AG comparison approach is the same as used in previous bridge applications [25], and works by identifying the maximum common subgraph (MCS) that exists between two graphs. When two structures are compared as graphs, a pair of elements can be considered to match if they are of the same element type (i.e., beam, slab etc) with matching attributes such as material, material properties and geometry. The largest matching portion of the graphs that is common to both structures is the MCS. This can be used to evaluate a similarity metric between two structures, which is intended to indicate the likely levels of achievable transfer between the two target structures [35].

Fig. 6 provides a demonstration of the AG comparison approach applied to two beam and slab bridges, namely B&S 1 and B&S 3. Fig. 6(a) shows a simplified graph representation of B&S 1 and Fig. 6(b) shows a simplified graph representation of B&S 3. The red nodes in the graphs represent regular elements (with their associated element attributes) and the blue nodes represent the ground elements, i.e., the support structures (with associated boundary information). The vertices between the nodes represent the interactions between the elements, including their associated information. Whilst the element attributes and relationship information are not visually presented in the graphs in Fig. 6, they are contained within the AG information for comparison. As the element attributes and relationship information are consistent between the beam and slab bridges (i.e., they both comprise reinforced concrete elements with fully fixed joints), the similarity metrics reflect the topological similarity between the bridge decks. Fig. 6(c) provides a visual demonstration of comparing the graphs from Fig. 6(a) and (b), where the unmatching portions of the graphs have been greyed out, and the matching portions are clearly visible.

The Jaccard Index [36], is used to calculate the similarity between the bridges as it is simple to implement and understand. In

(a)


```
{
    "version": "1.1.0",
    "name": "Truss-1",
    "population": "Bridge Decks",
    "timestamp": 1679422811000000000,
    "models": {
        "irreducibleElement": {
            "type": "grounded",
            "elements": [
                {
                    "name": "support-1-bearing-1",
                    "type": "ground"
                },
                {
                    "name": "deckslab",
                    "type": "regular",
                    "contextual": {
                        "type": "plate"
                    },
                    "geometry": {
                        "type": {
                            "name": "plate",
                            "type": {
                                "name": "rectangular"
                            }
                        }
                    },
                    "material": {
                        "type": {
                            "name": "metal",
                            "type": {
                                "name": "ferrousAlloy",
                                "type": {
                                    "name": "steel"
                                }
                            }
                        },
                        "symmetry": "isotropic",
                        "properties": [
                            {
                                "type": "density",
                                "unit": "kg/m^3",
                                "value": 7800
                            },
                            {
                                "type": "youngsModulus",
                                "unit": "MPa",
                                "value": 200000
                            }
                        ]
                    }
                },
```


(b)


```
"relationships": [
    {
        "name": "support-1-bearing-1-wall-1-upright-1",
        "type": "boundary",
        "elements": [
            {
                "name": "support-1-bearing-1"
            },
            {
                "name": "wall-1-upright-1"
            }
        ]
    },
    {
        "name": "deck-chord-1-wall-1-upright-1",
        "type": "joint",
        "nature": {
            "name": "static",
            "nature": {
                "name": "other"
            }
        },
        "elements": [
            {
                "name": "deck-chord-1"
            },
            {
                "name": "wall-1-upright-1"
            }
        ]
    },
```


Fig. 5. Sample of Truss 1 IE model: (a) element information, (b) relationship information.

essence, the Jaccard Index represents the size of the MCS obtained between two AGs of structures, relative to the size of the pair of AGs being compared. This can be written as:

$$J(A,B) = \frac{A \cap B}{A \cup B} = \frac{A \cap B}{|A| + |B| - |A \cap B|} \tag{1}$$

For the two beam and slab bridges compared in Fig. 6, there are 28 elements and 43 relationships in B&S 1, and 33 elements and 52 relationships in B&S 3. Fig. 6(c) shows that there are 28 matching elements and only 5 elements that do not match (two additional beams in B&S 3 and the three sections of diaphragm they connect to). Therefore:

$$J(B\&S1, B\&S2) = \frac{28}{28 + 33 - 29} = 0.85 \tag{2}$$

3.4. Results from comparing six bridges

When applied to a set of bridges, the results from the comparisons are presented in a table format. Each bridge is assigned a row and column of the table, and each cell of the table is the result of two bridges (i.e., one row and one column) being compared. Similarities of "0″ means no elements match, and "1" represents a perfect match between a pair of graphs (of structures). Fig. 7 presents the similarity metrics obtained from comparing the two truss and four beam and slab bridge decks. The diagonal line of "1" in the figure is composed of the similarity metrics between each model/graph compared with itself. The results for each comparison of bridge pairs are mirrored about the diagonal line, e.g., (A < B) = (B > A). The top-right side of the table has been faded out, and the bottom-left side of the table has been annotated to aid with narration of the results. For the comparisons involving the pair of truss footbridges (Fig. 7):

- The "1″ in Row 2, Column 1, circled in black, is the similarity metric between the two truss footbridges. The pair are identified as being topologically identical with the same number of elements in an identical arrangement.

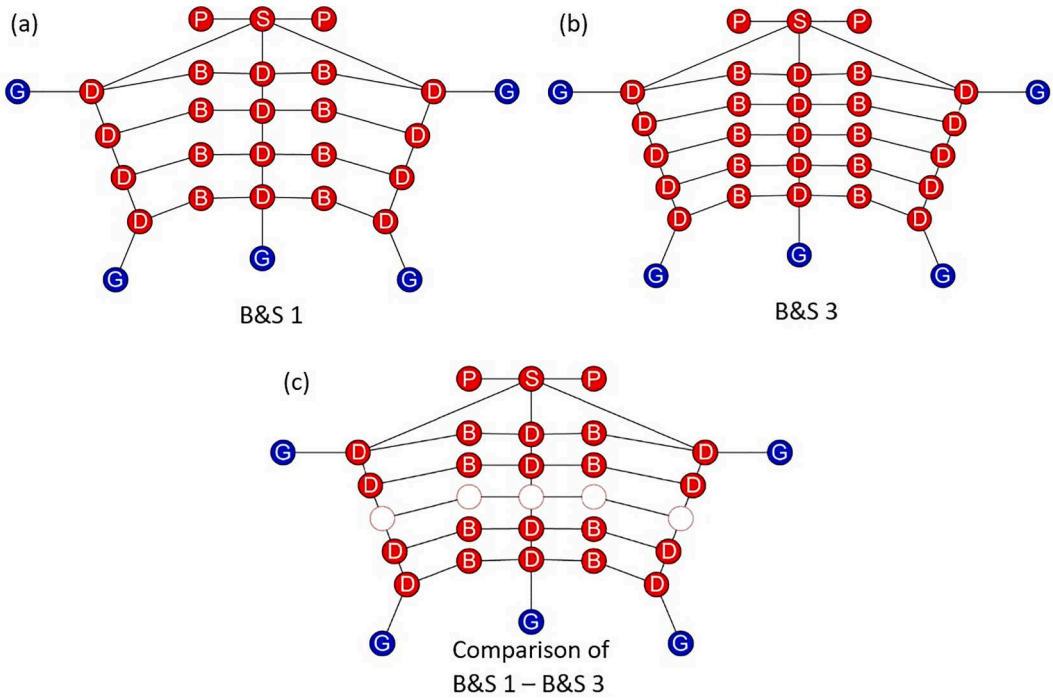

Fig. 6. Attributed Graphs, (a) B&S 1, (b) B&S 3, (c) comparison of B&S 1 and B&S 3.

- The black rectangle around Rows 3 – 6 and Columns 1 – 2 groups the similarity metrics obtained from comparing the four beam and slab bridges, B&S1 – B&S4, with the two truss footbridges. Both truss footbridges are identified as being entirely different to each of the beam and slab bridges with a consistent similarity of 0.01.

The beam and slab bridges feature a difference in the number of beams supporting the spans of each bridge deck (Section 3.2). The following observations are made from the resulting similarity metrics between the beam and slab bridges (Fig. 7):

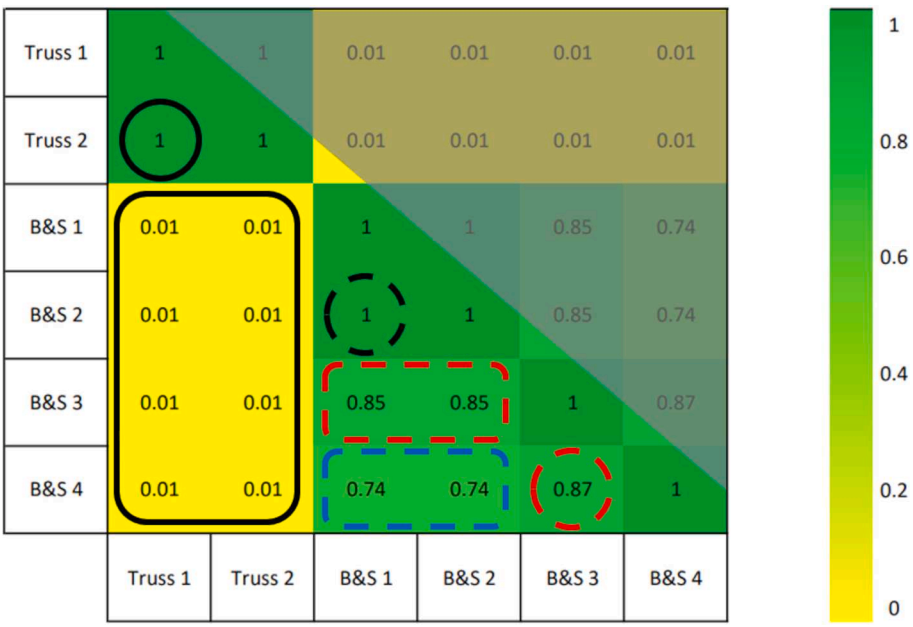

Fig. 7. Similarity metrics between bridge AGs.

- The black dashed circle in Row 4, Column 3 highlights the similarity metric from comparing B&S1 and B&S2. The pair of beam and slab bridges are identified as being topologically identical with the same number of elements in an identical arrangement.
- The red dashed rectangle in Row 5, Columns 3 and 4 groups the similarity metrics from comparing B&S3 (Row 5 and Column 5) with B&S1 and B&S2 (Rows and Columns 3 and 4, respectively). The additional beam in B&S3 results in a similarity metric of "0.85" when compared with either B&S1 or B&S2.
- The red dashed circle in Row 6, Column 5 outlines the similarity metric from comparing B&S4 (Row 6 and Column 6) with B&S3 (Row 5 and Columns 5). The additional beam in B&S4 results in a similarity metric of "0.87" when compared with B&S3.
- Finally, the blue dashed rectangle in Row 6, Columns 3 and 4 groups the similarity metrics from comparing B&S4 (Row 6 and Column 6) with B&S1 and B&S2 (Rows and Columns 3 and 4, respectively). The two additional beams in B&S4 results in a similarity metric of "0.74" when compared with either B&S1 or B&S2.

The consistent increasing number of elements making up the beam and slab bridge decks results in a consistent decreasing similarity metric between the bridge decks. Largely, the results in Fig. 7 are intuitive when considering the similarity (and differences) between the bridge decks and their constituent elements.

4. Data-collection campaign

This section details the data-collection campaign carried out for the six bridges for the purposes of assessing the similarity of the modal responses (of each bridge). Section 4.1 details the equipment used for all six modal tests. Section 4.2 presents the modal test set up, the data collected, and the mode shapes obtained for the two truss footbridges. Section 4.3 details the same for the beam and slab bridge mode tests. Fig. 7.

4.1. Equipment used

For each of the six bridges, the same Lord G-LINK-200 [37] accelerometers were used. These accelerometers are wireless and easy to deploy, and, with a 20-bit resolution and noise level of 25 $\mu g/\sqrt{Hz}$, they can capture ambient vibrations of bridges with a view to obtaining mode shapes and frequency–response data. The sensors were fixed to base plates that allowed for onsite levelling via levelling screws. Data for each test were collected using a laptop with SensorConnect software [38], via a wireless gateway/antenna. Fig. 8(a) shows a photo of one of the seven accelerometers deployed on one of the bridges. Fig. 8(b) shows a photo of the portable "monitoring station", that is, the laptop receiving live accelerations via gateway/antenna.

4.2. Truss bridge

4.2.1. Test set up

For the truss footbridge modal tests, the data were gathered in a single deployment of six accelerometers. The sensors were placed at quarter, mid and three-quarter spans at each side of the bridge (for both bridges) adjacent to the parapets. The sensor placement was designed to capture the vibration response from both sides of the bridge deck, allowing mode shapes to be estimated from the data collected. Fig. 9 shows a diagram of the sensor layout used for both truss footbridges. The six sensor locations are marked as S1-S6 in the Figure.

4.2.2. Data collected

The vibrations for the test were mainly induced by traffic passing under the bridge and from heel drops performed at quarter, mid and three-quarter spans of the bridge. Overall, approximately 19 min of data were collected, and this was found to be sufficient to capture dynamic responses from the truss bridges. A linear detrend was used in Matlab [39] for preprocessing of the acceleration

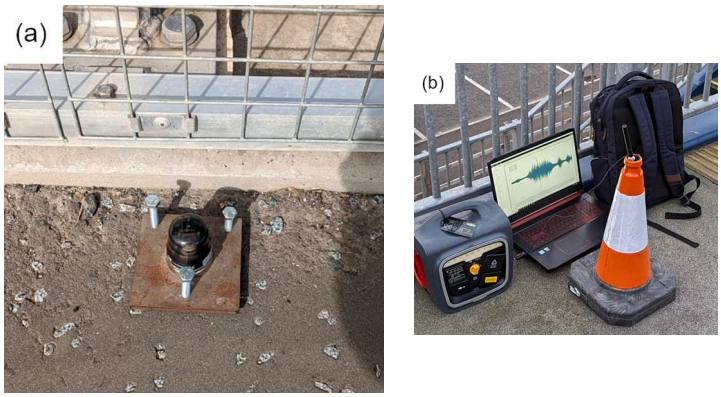

Fig. 8. Testing equipment: (a) accelerometer on baseplate as deployed on the bridges, (b) monitoring station with laptop and gateway/antenna.

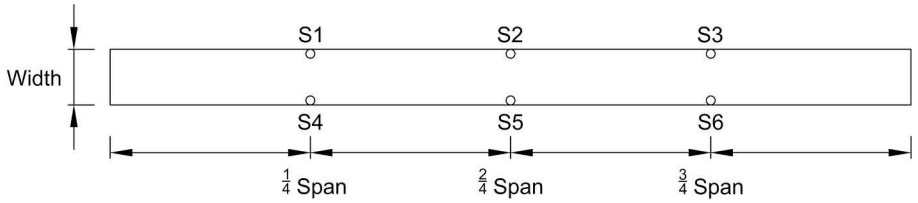

Fig. 9. Plan view of truss bridge deck with test points annotated.

signals. Fig. 10(a)–(c) shows the detrended acceleration timeseries measured on the first truss footbridge (Truss 1). Fig. 10(a) shows the acceleration from sensors S1 and S4 (red and blue-dashed signals, respectively). Fig. 10(a) shows a zoomed-in view of one of the vehicle-induced vibrations (upper insert, blue outline) and a set of three heel drop-induced excitations recorded by S1 and S4 at quarter span (lower insert, red outline). Fig. 10(b) shows the acceleration from sensors S2 and S5 (red and blue-dashed signals, respectively) and Fig. 10(c) shows the acceleration from sensors S3 and S6 (red and blue-dashed signals, respectively). Fig. 10(d)–(f) shows the power spectral density (PSD) estimate obtained from the accelerations in Fig. 10(a)–(c) respectively, using MATLAB [40]. Five peaks of interest have been labelled (1 – 5), where the fifth frequency peak (close to 30 Hz) was the smallest in magnitude. An enhanced view of the fifth peak is shown as an insert in Fig. 10(d).

4.2.3. Modal analysis

Operational modal analysis (OMA) for each bridge was carried out using bespoke MODAL software that utilises the NExT/ERA method [41,42]. The software has been described and demonstrated elsewhere [43,44], and was selected here for its compatibility with assessing ambient vibration data from bridge structures. For both truss footbridges, the software produced a clean set of modes, corresponding to the frequencies identified in the PSD estimates. Fig. 11 presents the mode shapes (and associated frequencies) obtained for both truss footbridges in a table format.

Five distinct modes labelled M1 – M5 (rows 1 – 5 in Fig. 11) were identified from the accelerations from both Truss 1 and Truss 2 (columns 1 and 2, respectively). Each of the identified modes corresponds with a frequency peak identified from the PSD estimates from the acceleration data (Fig. 10). Modes M1, M3 and M4 are longitudinal bending modes, with the order increasing with frequency. Modes M2 and M5 present as torsion of the deck. For the modes M1 – M3, the modal amplitudes from the Truss 2 modes are less symmetrical than from Truss 1. The reason for this effect is unknown; however, the higher-order modes (M4 and M5) appear less affected and there is a closer similarity between the two bridges.

4.3. Beam and slab bridges

4.3.1. Test set-up

The equipment used for the beam and slab bridge modal tests was the same as used for the truss footbridges but for the inclusion of a seventh accelerometer as a reference sensor. The beam and slab bridges are two spans each and are substantially wider than either of the truss footbridges. As a result, the modal test was carried out in four 'swipes' per bridge. Fig. 12 is a plan view of the typical beam and slab bridge test layout. In Swipe 1, sensors were at locations S1 – S6. In Swipe 2, sensors were at locations S7 – S12. In Swipe 3, sensors were at locations S13 – S18. In Swipe 4, sensors were at locations S19 – S24. A seventh sensor was used as a reference sensor to normalise the data from all four swipes in post processing. The reference sensor was located between the mid and three-quarter span location of Span 1, adjacent to the parapet (SR located equidistant between S8 and S9). Once deployed, the reference sensor remained in location until the testing was complete for the bridge. The sensor locations were selected to capture the dynamic response for the whole bridge deck, with transverse sensor placements restricted to the footpaths/verges of the bridges.

4.3.2. Data collected

The excitation for the beam and slab bridges was largely from live traffic crossing the bridge. As the bridges selected are in a rural location with relatively low volumes of traffic, the durations for each of the four swipes of the mode test (per bridge) ranged from 40 to 80 min per part-test to gather enough excitations in the recorded data for analysis. The raw accelerations for each swipe, and each bridge, were detrended using a linear detrend in Matlab. Fig. 13 shows the detrended acceleration data from Swipe 1 of the first beam and slab bridge (B&S1) modal test. Fig. 13(a) shows the quarter-span accelerations (S1 and S4). The insert in the Figure shows the response recorded from a single vehicle crossing the bridge. Fig. 13(b) is the mid-span accelerations (S2 and S5). Fig. 13(c) is the three-quarter span accelerations (S3 and S6). Fig. 13(d) is the reference sensor accelerations recorded during the same period as Fig. 13(a)–(c). Fig. 13(e)–(h) show the frequency–response spectra obtained from the signals in Fig. 13(a)–(d), respectively. Four prominent frequencies have been identified and labelled 1 – 4 in Fig. 13(e)−(h), that were common across all four swipes of the modal test.

4.3.3. Modal analysis

The OMA of the beam and slab bridges was carried out using the same software as for the two truss footbridges, with a minor change in the procedure. As the tests were carried out in four swipes, the reference sensor data are required to normalise the data (using a cross-power matrix) for each swipe of the test, and therefore position on the bridge. For each of the four beam and slab bridges, clean

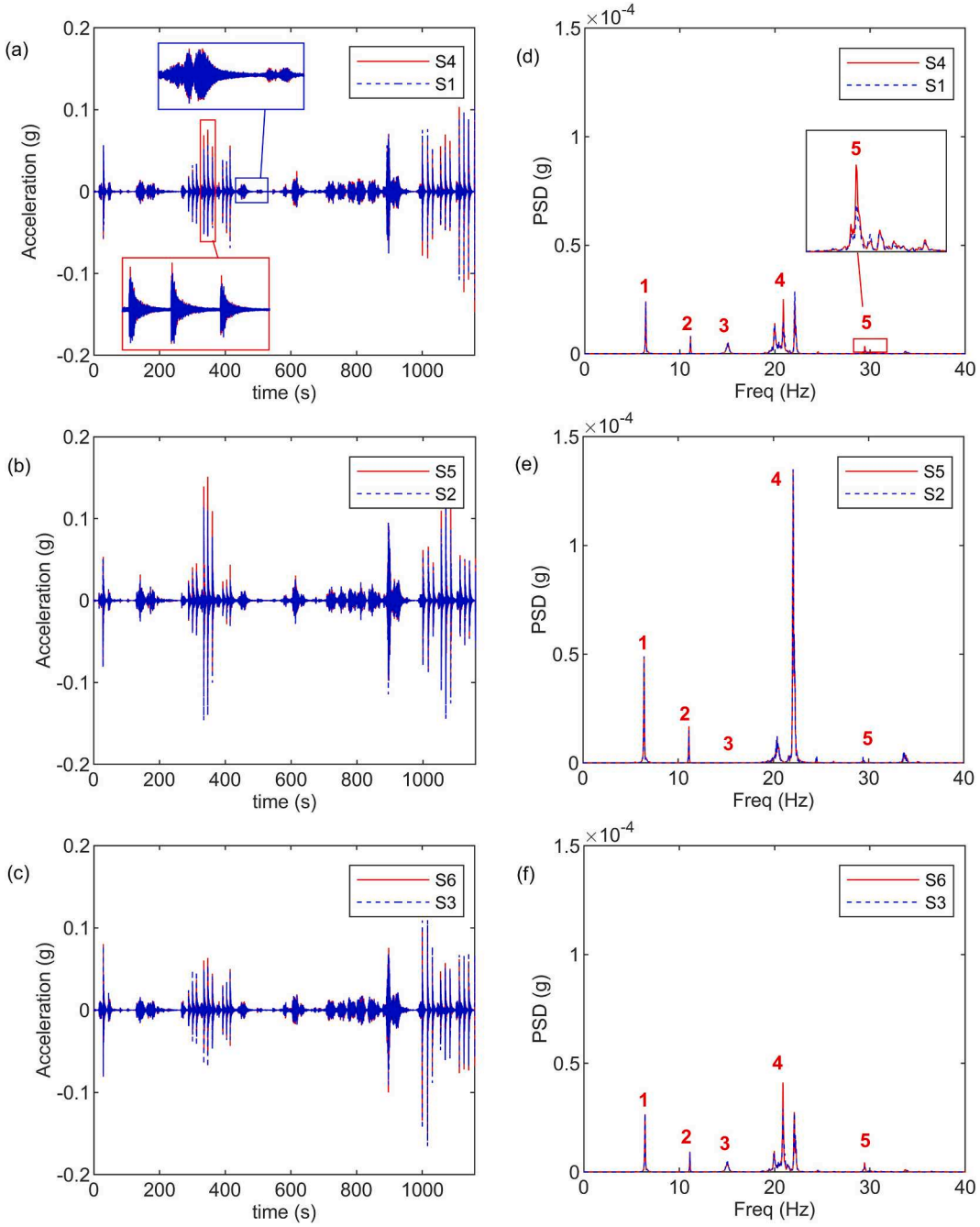

Fig. 10. Vibration response data from Truss 1, (a) ¼-span accelerations, (b) mid-span accelerations, (c) ¾-span accelerations, (d) ¼-span PSD estimate, (e) mid-span PSD estimate, (f) ¾-span PSD estimate.

sets of modes were identified that correlated with frequency peaks observed in the PSD responses from each bridge (Fig. 13). Fig. 14 presents the four Modes (M1 – M4) identified from the beam and slab bridges (B&S1 – B&S4), with each row of the figure presenting the modes for a given bridge.

From the figure, the following observations can be made:

- For the first three beam and slab bridges, B&S1 – B&S3 (presented in rows 1 – 3 of Fig. 14) the first two modes (M1 and M2) both present with longitudinal bending of the bridge deck, but with a different phase. The second mode (M2) was not identified from B&S4 analysis.
- For all 4 bridges the third mode (M3) appears as a torsion mode shape in Span 1 with appreciably more subtle response in Span 2.

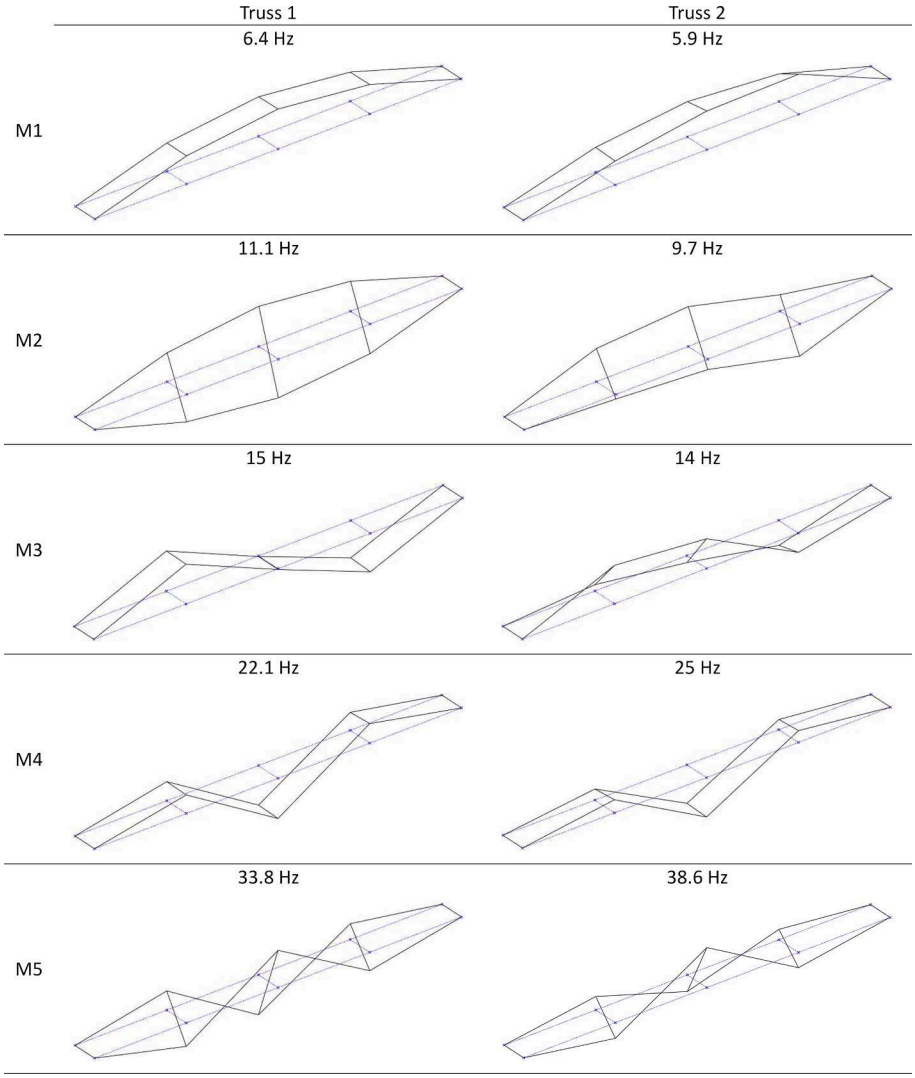

Fig. 11. Truss bridge mode responses for Truss 1 and 2, modes M1 – M5.

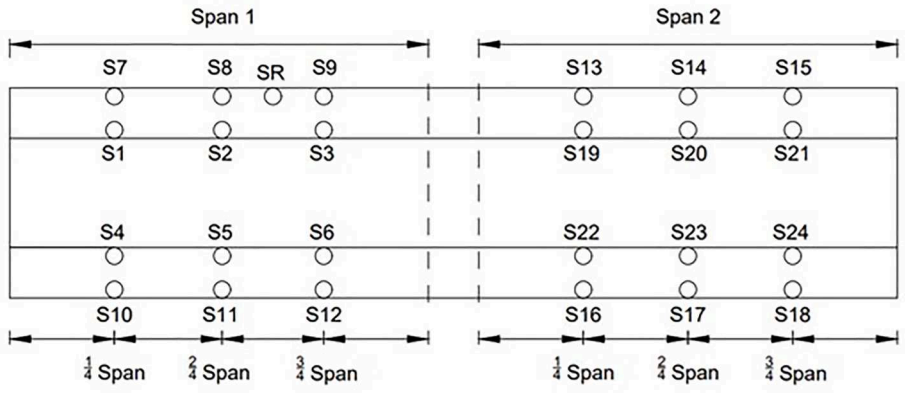

Fig. 12. Plan view of beam and slab bridge test set up.

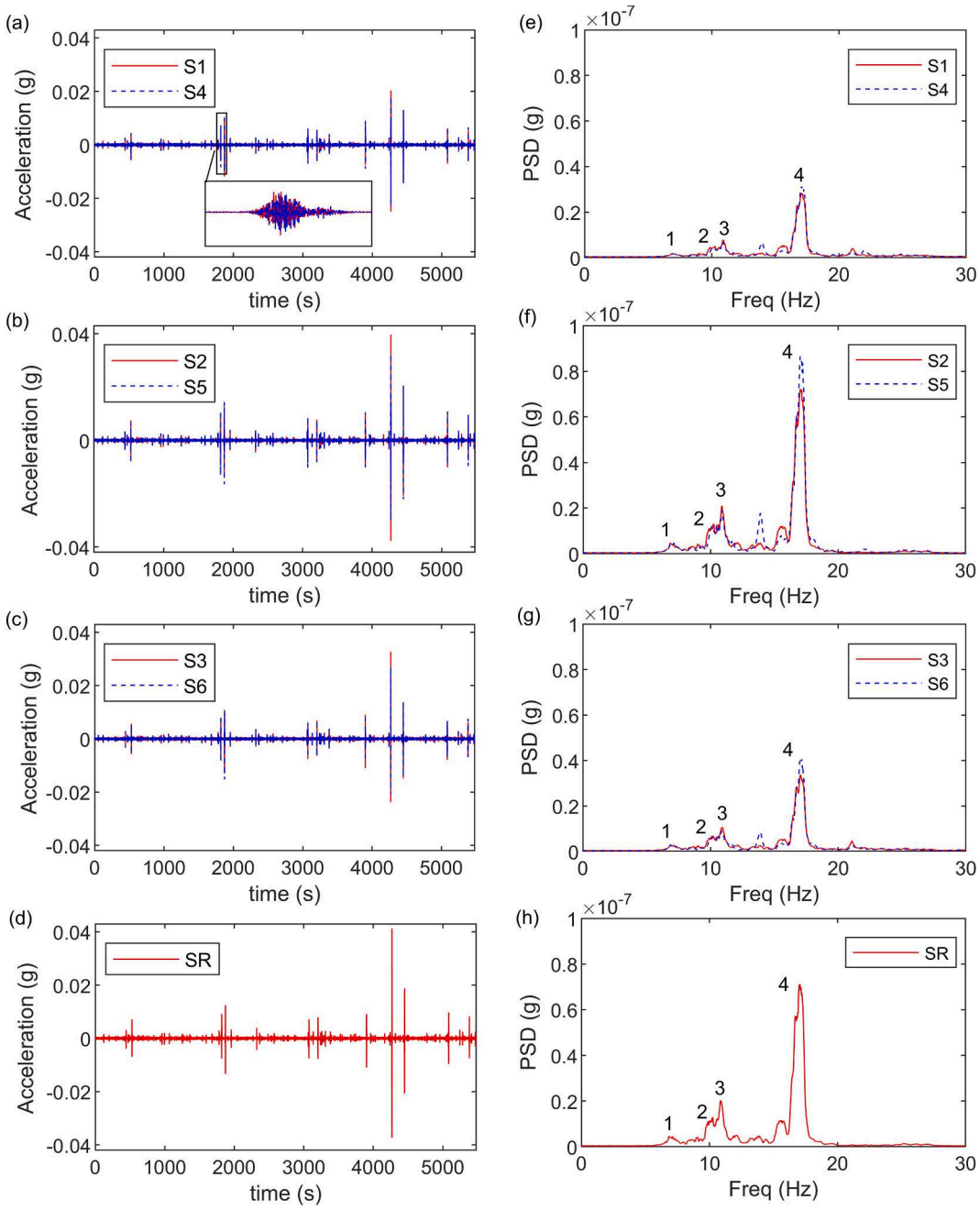

Fig. 13. Vibration response data from B&S1: (a) ¼-span acceleration, (b) mid-span accelerations, (c) ¾-span accelerations, (d) Reference sensor accelerations, (e) ¼-span PSD estimates, (f) mid-span PSD estimates, (g) ¾-span PSD estimates, (h) Reference sensor PSD estimates.

- For all 4 bridges the fourth mode (M4) appears as a bending mode but with significant variation in the modal amplitude transversely across the structure. The sensors at the kerb and parapet locations were only approximately 2.5 m apart, leaving approximately 8 m – 11 m of carriageway with no sensor placements. For both B&S3 and B&S4, the mode presented in one span only.

5. Graph-space distances and bridge response variations

This section reviews the similarity metrics between the six bridges, considering the dynamic responses obtained from the respective bridges. The Modal Assurance Criterion (MAC) is used as it is a statistical indicator that is sensitive to large differences between mode shapes, and less sensitive to subtle differences [45]. The MAC results range from 0 to 1, where 0 means there is no similarity between

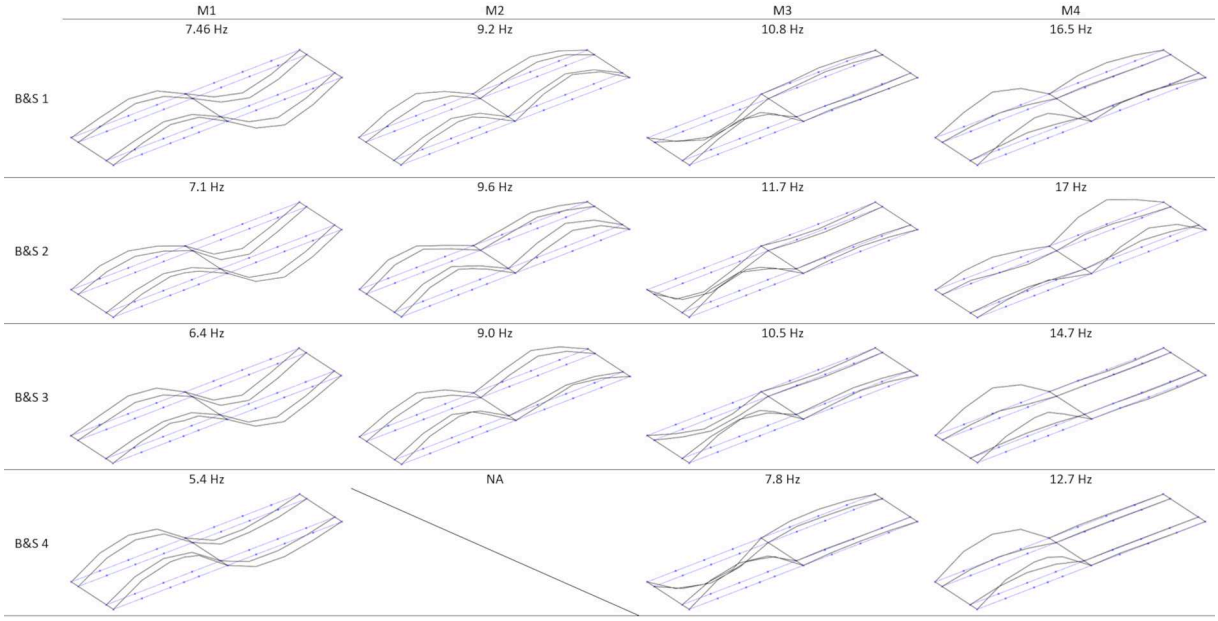

Fig. 14. Beam and slab bridge mode responses for B&S 1 – 4, modes M1 – M4.

two modes, and 1 means the pair of modes are identical. This similarity scale of 0 to 1 is consistent with the numerical scale used for comparing structural topologies (see Fig. 7). Section 5.1 discusses the MACs and similarity metric between the two nominally similar truss footbridges (Fig. 7 and Fig. 11). Section 5.2 discusses the MACs and similarity metrics between the four similar beam and slab bridges (Fig. 7 and Fig. 14). Finally, Section 5.3 comments on the comparison of responses and similarity metrics between bridges of the same and different types.

5.1. Truss bridges

Based on engineering judgement, the two truss footbridges appear very similar and resulted in a similarity of 1.0 when compared as AGs (Fig. 7). The mode shapes identified for each bridge were largely similar also (Fig. 11). Fig. 15 presents the MAC results from comparing Truss 1 and Truss 2 modes. Three of the five modes, M1, M4 and M5 are confirmed as being very similar with high MAC values (0.93, 0.89 and 0.89, respectively). Two of the modes identified from Truss 2, M2 and M3, present with asymmetrical modal amplitudes that do not feature in the modes from Truss 1. This disparity in the modal amplitudes results in MAC values of 0.58 and 0.64 for modes M2 and M3, respectively.

From an engineering perspective, the similarity between the mode shapes make sense as the bridges are constructed with near identical arrangements (i.e., the mode shapes are sensitive to the topology of the elements comprising the structure). The high MAC values between the two bridges' MPs are in line with visual observations between the modes from the two bridges. In broad terms, the results give confidence that the high similarity metric is indeed reflective of meaningful structural similarity. That is, the two truss bridges are similar enough that there could potentially be valuable SHM inferences that could be made between the set of bridges.

5.2. Beam and slab bridges

The set of four beam and slab bridges feature more topological variation than the two truss footbridges. The first two beam and slab bridges, B&S1 and B&S2, have the same number of elements in the same formation/arrangement. B&S3 is wider than B&S1 and B&S2,

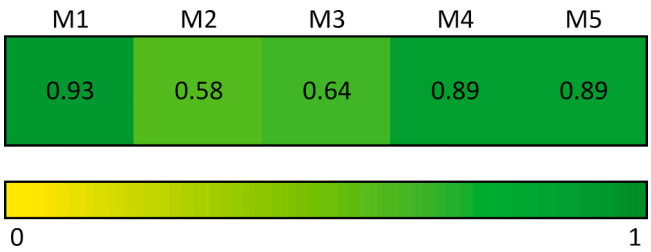

Fig. 15. MAC results between Truss 1 and Truss 2 modes M1 – M5.

and B&S4 is wider than B&S3, featuring additional precast beams per span (Fig. 4). The increased variation results in decreased similarity metrics (Fig. 7). Despite the variations, there is a high similarity between the set of mode shapes observed in Fig. 14. Fig. 16 presents the MAC results from comparing each of the four modes (M1 – M4) between the set of beam and slab bridges. The tables of results have been annotated to reflect the similarity metrics presented in Fig. 7. (Note that Fig. 16(b) presents the MAC values for mode 2 between the bridges and only has a 3x3 grid of results as mode 2 did not present in B&S4, see Fig. 14).

The main variations between B&S1 and B&S2 are the span lengths which are not captured by the IE models. The bridges feature the same number of elements in a similar construction resulting in a similarity metric of 1.0 (Fig. 7), as in the truss footbridge comparisons. The MAC values between B&S1 and B&S2 are annotated with a black dashed circle in Fig. 16. Three of the four modes, M1, M3 and M4 (Fig. 16(a), (b) and (d)) show a high similarity (0.93, 0.79 and 0.94, respectively) between the two bridges. There appears to be more variation in mode M3 (Fig. 16(c)), with a MAC value of 0.61. The similarity between the two bridges' MPs gives confidence that the high similarity metric ('1.0′ in Fig. 7) is reflective of meaningful structural similarity.

The third beam and slab bridge (B&S 3), compared with B&S 1 and B&S 2 (in graph form), results in a similarity metric of 0.86 (Fig. 7); this makes sense, as the bridge features an additional beam per span and is wider than B&S1 and B&S2, reducing the topological similarity of the bridge decks. The MPs from the bridge are largely similar to the first two beam and slab bridges when considering the mode shapes in Fig. 14, and MAC values in Fig. 16 (outlined with red dashed rectangles). Modes M1 and M2 result in high MAC values when comparing B&S3 with B&S1 and B&S2, ranging from 0.81 to 0.96 (see the red dashed rectangles in Fig. 16(a) & (b). Modes M3 and M4 show larger variations, with MAC values ranging from 0.66 to 0.82 (see the red dashed rectangles in Fig. 16(c) & (d). The slightly lower similarity metric from comparing B&S3 with B&S1 and B&S2 in Fig. 7 appears to be consistent with a slightly greater variation between the modes of the bridges.

The fourth beam and slab bridge (B&S 4) results in a similarity metric of 0.88 when compared with B&S3, and 0.75 when compared with B&S1 and B&S2 (Fig. 7). The structural difference between B&S4 and the other bridges indicated by the graph similarity scores are consistent with the observed differences between the mode shapes. B&S4 was the only bridge not to feature the mode M2, longitudinal bending with both spans being in phase with one another. That said, despite the differences, there is still a relatively high level of similarity between the mode shapes of B&S4 and the mode shapes of B&S1-3. The MAC results from comparing B&S4 with B&S1 and B&S2 are outlined with blue dashed rectangles in Fig. 16 and values range from 0.64 to 0.81. The results from the comparison with B&S3 are outlined with red dashed circles in Fig. 16 and values range from 0.76 to 0.87. Overall, B&S4 mode shapes are identified as being closer to B&S3 than either B&S1 or B&S2. The similarity metrics from Fig. 7 appear largely reflective of the meaningful similarities between the bridges, as verified with the MAC values in Fig. 16.

5.3. *Bridges of the same and different types*

The similarity metrics between bridges of the same type appear to reflect the level of similarity observed experimentally as MPs (i.e., mode shapes). The results suggest that some level of insight may be sharable between the structures for SHM purposes. The similarity metrics between the bridges of different types appear to reflect the level of the difference observed between the truss and beam and slab bridge responses. With similarities of 0.01 (Fig. 7), the substantial difference between the bridge responses (Fig. 11 and Fig. 14) is entirely as would be expected. Collectively, the results indicate that the graph comparison approach is credibly assessing the similarity between bridges of the same and different types.

6. Conclusions

PBSHM is a new approach to SHM that has the potential to make a significant impact to the bridge management and SHM communities. The IE model schema and AG comparison approach has been newly introduced to real bridge structures, with applications to date only qualified using engineering judgement i.e., no quantitative data have been used to make judgement on the calculated similarity metrics. Therefore, this paper expands on the previous work and compares the dynamic responses of a set of six bridges. The MPs from two truss footbridge decks and four beam and slab bridge decks are compared relative to similarity between the same bridge-deck structures. The specific conclusions of the paper are outlined below:

1. Bridges identified as entirely different, namely the truss and beam and slab bridges featured very different MPs, validating the low similarity metrics evaluated.
2. For bridges identified as notionally identical in topology, namely the two truss bridges (Truss 1 and Truss 2), and then two beam and slab bridges (B&S1 and B&S2), the MPs of the bridges are very similar, justifying the high similarity metrics between the bridges.
3. For bridges that feature subtle variations in topology, namely the four beam and slab bridges (B&S1 – B&S4), the similarity metrics between the bridges reflect the similarities observed between the bridge deck MPs. That is, as the similarity metrics between beam and slab bridge decks decrease, the similarity between the MPs also decreases.

Bridge decks are essentially plate structures; hence, the mode shapes identified in this paper manifest mostly as 'plate' mode shapes with fairly ordinary bending and torsion forms. In broad terms, the MACs cannot get too low because of the core similarity between the mode shapes of plate structures. However, IE models can include elements that are peripheral to the bridge deck plate structure (substructure and superstructure) which can reduce the resolution of the similarity metric identified between two graphs (of structures). Even if the truss and beam and slab bridge modes had been compared, they would have yielded a more comparable MAC than

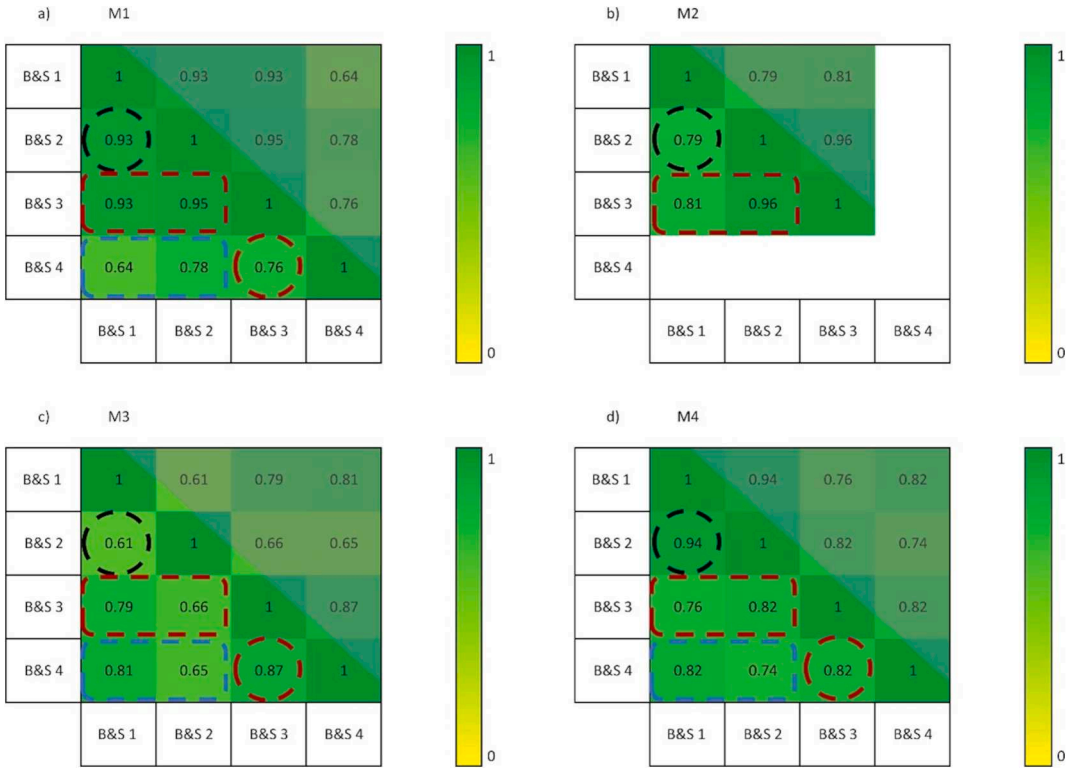

Fig. 16. MAC between four beam and slab bridge modes: (a) M1, (b) M2, (c) M3 and (d) M4.

the very low '0.1′ similarity metric identified between the different bridge types. However, that is not to say the modal information would necessarily be directly transferrable. Therefore, if IE models are to be 'problem-driven', there still remains questions of:

- What knowledge is being sought for transfer?
- What elements (from substructures and superstructures) should be described within the IE models to reflect the extents of the datasets being considered? And,
- What detail should be included in the element descriptions that is relevant to the datasets being considered?

The bridge deck constructions considered were relatively common, indicating there could be a substantial pool of bridges that would be identifiable, and potentially manageable, as a population of bridges with the ability to share learning. Alternatively, for multiple span bridges, where span construction is consistent and so are the nominal span responses, there could be scope to monitor the various spans (and supports) relative to one another, or relative to a data model trained from the community of span models. The similarity metrics presented in this paper were effective in predicting the similarity between dynamic bridge responses of pairs of bridges, reflecting the potential for SHM information to be transferrable between the pairs.

Whilst the results in this work are encouragingly positive, it was primarily the mode shape responses that were considered between bridge decks and the set of bridges was relatively small. That is, it remains unknown if the same problem driven modelling approach would be as effective for evaluating the similarity between other bridge decks/parts of bridges, or for other bridge deck responses, such as static load response (e.g., rotation/displacement). Particularly considering larger bridges, such as long span suspension bridges, further investigation would be required as to what datasets would be comparable between these bridges. However, there would need to be consideration as to what elements are relevant to those datasets, as the graph comparison resolution is sensitive to the size of the graphs being compared, and oversimplification or overcomplication of IE models could result in misleading similarity metrics. That said, the work in this paper justifies the further investigation of how we can compare bridges for similarity, and what information can then be shared between similar bridges.

CRediT authorship contribution statement

Andrew Bunce: Writing – original draft, Visualization, Resources, Project administration, Methodology, Investigation, Formal analysis, Data curation, Conceptualization. **Daniel S. Brennan:** Writing – review & editing, Software. **Alan Ferguson:** Investigation, Data curation. **Connor O'Higgins:** Investigation, Data curation. **Su Taylor:** Writing – review & editing, Supervision. **Elizabeth J Cross:** Writing – review & editing, Supervision. **Keith Worden:** Writing – review & editing, Supervision, Software, Conceptualization.

James Brownjohn: Writing – review & editing, Validation, Software. **David Hester:** Writing – review & editing, Validation, Supervision, Resources, Project administration, Conceptualization.

Declaration of competing interest

The authors declare that they have no known competing financial interests or personal relationships that could have appeared to influence the work reported in this paper.

Data availability

Data will be made available on request.

Acknowledgements

The authors would like to thank Department for Infrastructure (Northern Ireland) for permission to use their bridges, in particular Kris Campbell for the support in the field testing. The research and work leading to these results was supported by EPSRC DTP grant EP/R513118/1 and the Established Career Fellowship EP/R003645/1. It also received support from the UK Engineering and Physical Sciences Research Council (EPSRC) via the ROSEHIPS project (Grant EP/W005816/1). For open access, the authors have applied a Creative Commons Attribution (CC BY) licence to any Author Accepted Manuscript version arising.

References

[1] P. Desnerck, J.M. Lees, P. Valerio, N. Loudon, C.T. Morley, Inspection of RC half-joint bridges in England: analysis of current practice, Proceedings of the Institution of Civil Engineers - Bridge Engineering 171 (4) (Dec. 2018) 290–302, https://doi.org/10.1680/jbren.18.00004.
[2] B. Bakht, A. Mufti, Evaluation of one hundred and one instrumented bridges suggests a new level of inspection should be established in the bridge design codes, J Civ Struct Health Monit 8 (1) (2018) 3, https://doi.org/10.1007/s13349-017-0256-1.
[3] M. Flah, I. Nunez, W. Ben Chaabene, and M. L. Nehdi, "Machine Learning Algorithms in Civil Structural Health Monitoring: A Systematic Review," Archives of Computational Methods in Engineering, no. 0123456789, 2020, doi: 10.1007/s11831-020-09471-9.
[4] I. Antoniadou, N. Dervilis, E. Papatheou, A. E. Maguire, and K. Worden, "Aspects of structural health and condition monitoring of offshore wind turbines," Philosophical Transactions of the Royal Society A: Mathematical, Physical and Engineering Sciences, vol. 373, no. 2035, 2015, doi: 10.1098/rsta.2014.0075.
[5] K. Worden, E.J. Cross, N. Dervilis, E. Papatheou, I. Antoniadou, Structural Health Monitoring: from Structures to Systems-of-Systems, IFAC-PapersOnLine 48 (21) (2015) 1–17, https://doi.org/10.1016/j.ifacol.2015.09.497.
[6] N. Dervilis, A.C.W. Creech, A.E. Maguire, I. Antoniadou, R.J. Barthorpe, K. Worden, An SHM View of a CFD Model of Lillgrund Wind Farm, Appl. Mech. Mater. 564 (Jun. 2014) 164–169, https://doi.org/10.4028/www.scientific.net/AMM.564.164.
[7] E. Papatheou, N. Dervilis, A.E. Maguire, I. Antoniadou, K. Worden, A Performance Monitoring Approach for the Novel Lillgrund Offshore Wind Farm, IEEE Trans. Ind. Electron. 62 (10) (2015) 6636–6644, https://doi.org/10.1109/TIE.2015.2442212.
[8] L.A. Bull, et al., Foundations of population-based SHM, Part I: Homogeneous populations and forms, Mech Syst Signal Process 148 (2021) 107141, https://doi.org/10.1016/j.ymssp.2020.107141.
[9] G. Tsialiamanis, N. Dervilis, D.J. Wagg, K. Worden, Towards a population-informed approach to the definition of data-driven models for structural dynamics, Mech Syst Signal Process 200 (Oct. 2023) 110581, https://doi.org/10.1016/j.ymssp.2023.110581.
[10] L.A. Bull, et al., Bayesian modelling of multivalued power curves from an operational wind farm, Mech Syst Signal Process 169 (Apr. 2022), https://doi.org/10.1016/j.ymssp.2021.108530.
[11] W. Lin, K. Worden, A. Eoghan Maguire, E.J. Cross, Towards Population-Based Structural Health Monitoring, Part VII: EOV Fields – Environmental Mapping, in: Conference Proceedings of the Society for Experimental Mechanics Series, 2021, pp. 297–304, https://doi.org/10.1007/978-3-030-47717-2_31.
[12] W. Lin, K. Worden, A.E. Maguire, E.J. Cross, "A mapping method for anomaly detection in a localized population of structures", Data-Centric, Engineering 3 (7) (2022) Aug, https://doi.org/10.1017/dce.2022.25.
[13] P. Gardner, L.A. Bull, J. Gosliga, N. Dervilis, K. Worden, Foundations of population-based SHM, Part III: Heterogeneous populations – Mapping and transfer, Mech Syst Signal Process 149 (2021) 107142, https://doi.org/10.1016/j.ymssp.2020.107142.
[14] Z. Wang, Z. Dai, B. Poczos, and J. Carbonell, "Characterizing and avoiding negative transfer," Proceedings of the IEEE Computer Society Conference on Computer Vision and Pattern Recognition, vol. 2019-June, pp. 11285–11294, 2019, doi: 10.1109/CVPR.2019.01155.
[15] K. Worden, et al., A Brief Introduction to Recent Developments in Population-Based Structural Health Monitoring, Front Built Environ 6 (September) (2020) 1–14, https://doi.org/10.3389/fbuil.2020.00146.
[16] P. Gardner, L.A. Bull, N. Dervilis, K. Worden, On the application of kernelised Bayesian transfer learning to population-based structural health monitoring, Mech Syst Signal Process 167 (Mar. 2022), https://doi.org/10.1016/j.ymssp.2021.108519.
[17] P. Gardner, X. Liu, K. Worden, On the application of domain adaptation in structural health monitoring, Mech Syst Signal Process 138 (2020) 106550, https://doi.org/10.1016/j.ymssp.2019.106550.
[18] L.A. Bull, et al., On the transfer of damage detectors between structures: An experimental case study, J Sound Vib 501 (Jun. 2021), https://doi.org/10.1016/j.jsv.2021.116072.
[19] T.A. Dardeno, L.A. Bull, R.S. Mills, N. Dervilis, K. Worden, Modelling variability in vibration-based PBSHM via a generalised population form, J Sound Vib 538 (Nov. 2022), https://doi.org/10.1016/j.jsv.2022.117227.
[20] S. Teng, X. Chen, G. Chen, L. Cheng, Structural damage detection based on transfer learning strategy using digital twins of bridges, Mech Syst Signal Process vol. 191, no. January (2023) 110160, https://doi.org/10.1016/j.ymssp.2023.110160.
[21] K.J. Vamvoudakis-Stefanou, J.S. Sakellariou, S.D. Fassois, Random vibration response-only damage detection for a set of composite beams, in: Proceedings of ISMA 2014 - International Conference on Noise and Vibration Engineering and USD 2014 - International Conference on Uncertainty in Structural Dynamics, 2014, pp. 3839–3854.
[22] K.J. Vamvoudakis-Stefanou, S.D. Fassois, Vibration-based damage detection for a population of nominally identical structures via Random Coefficient Gaussian Mixture AR model based methodology, Procedia Eng 199 (2017) 1888–1893, https://doi.org/10.1016/j.proeng.2017.09.123.
[23] K. Worden, D. Hester, A. Bunce, J. Gosliga, "when Is a Bridge Not an Aeroplane ?" no. July (2021) 1–8.
[24] G. Delo, et al., "When is a Bridge Not an Aeroplane? Part II: A Population of Real, Structures" (2023) 965–974, https://doi.org/10.1007/978-3-031-07258-1_97.
[25] J. Gosliga, D. Hester, K. Worden, A. Bunce, On Population-based structural health monitoring for bridges, Mech Syst Signal Process vol. 173, no. January (2022) 108919, https://doi.org/10.1016/j.ymssp.2022.108919.
[26] D.S. Brennan, J. Gosliga, P. Gardner, R.S. Mills, K. Worden, On the application of population-based structural health monitoring in aerospace engineering, Front Robot AI 9 (2022), https://doi.org/10.3389/frobt.2022.840058.

[27] G. Tsialiamanis, C. Mylonas, E. Chatzi, N. Dervilis, D.J. Wagg, K. Worden, Foundations of population-based SHM, Part IV: The geometry of spaces of structures and their feature spaces, Mech Syst Signal Process 157 (Aug. 2021), https://doi.org/10.1016/j.ymssp.2021.107692.
[28] J. Gosliga, P.A. Gardner, L.A. Bull, N. Dervilis, K. Worden, Foundations of Population-based SHM, Part II: Heterogeneous populations – Graphs, networks, and communities, Mech Syst Signal Process 148 (2021) 107144, https://doi.org/10.1016/j.ymssp.2020.107144.
[29] D. S. BRENNAN, J. GOSLIGA, E. J. CROSS, and K. WORDEN, "ON IMPLEMENTING AN IRREDUCIBLE ELEMENT MODEL SCHEMA FOR POPULATION-BASED STRUCTURAL HEALTH MONITORING," in Proceedings of the 13th International Workshop on Structural Health Monitoring, Destech Publications, Inc., Mar. 2022. doi: 10.12783/shm2021/36342.
[30] D. S. Brennan, T. J. Rogers, E. J. Cross, and K. Worden, "On Quantifying the Similarity of Structures via a Graph Neural Network for Population-based Structural Health Mon-itoring.".
[31] C. Bron, J. Kerbosch, Algorithm 457: finding all cliques of an undirected graph, Commun ACM 16 (9) (Sep. 1973) 575–577, https://doi.org/10.1145/362342.362367.
[32] Y. Cao, T. Jiang, T. Girke, A maximum common substructure-based algorithm for searching and predicting drug-like compounds, Bioinformatics 24 (13) (Jul. 2008) i366–i374, https://doi.org/10.1093/bioinformatics/btn186.
[33] I. Koch, Enumerating all connected maximal common subgraphs in two graphs, www.elsevier.com/locate/tcs, [Online]. Available, 2001.
[34] R. Diestel, Graph Theory (Graduate Texts in Mathematics), 3rd ed., Springer-Verlag, New York, 2006.
[35] P. Gardner, L.A. Bull, J. Gosliga, J. Poole, N. Dervilis, K. Worden, A population-based SHM methodology for heterogeneous structures: Transferring damage localisation knowledge between different aircraft wings, Mech Syst Signal Process 172 (Jun. 2022), https://doi.org/10.1016/j.ymssp.2022.108918.
[36] P. Jaccard, "Etude comparative de la distribution florale dans une portion des alpes et des jura," Bulletin del la Societe Vaudoise des Sciences Naturelles, no. 37, 1901.
[37] "Lord G-LINK-200." [Online]. Available: https://www.microstrain.com/wireless-sensors/g-link-200.
[38] "SensorConnect Software." [Online]. Available: https://www.microstrain.com/software/sensorconnect.
[39] "MATLAB - Detrend function." [Online]. Available: https://uk.mathworks.com/help/ident/ref/iddata.detrend.html.
[40] "MATLAB - PWelch function." [Online]. Available: https://uk.mathworks.com/help/signal/ref/pwelch.html.
[41] J.M. Caicedo, Practical guidelines for the natural excitation technique (next) and the eigensystem realization algorithm (era) for modal identification using ambient vibration, Exp Tech 35 (4) (Jul. 2011) 52–58, https://doi.org/10.1111/j.1747-1567.2010.00643.x.
[42] C. Gentile, N. Gallino, Ambient vibration testing and structural evaluation of an historic suspension footbridge, Adv. Eng. Softw. 39 (4) (Apr. 2008) 356–366, https://doi.org/10.1016/j.advengsoft.2007.01.001.
[43] D. Hester, K. Koo, Y. Xu, J. Brownjohn, M. Bocian, Boundary condition focused finite element model updating for bridges, 2018, p. 109514, Eng Struct 198 (September) (2019), https://doi.org/10.1016/j.engstruct.2019.109514.
[44] J. M. W. Brownjohn, H. Hao, and T.-C. Pan, "Assessment of structural condition of bridges by dynamic measurements Applied Research Report RG5/97," no. January, p., 2001, [Online]. Available: http://vibration.ex.ac.uk/doc/10174972.pdf.
[45] M. Pastor, M. Binda, and T. Harčarik, "Modal assurance criterion," in Procedia Engineering, Elsevier Ltd, 2012, pp. 543–548. doi: 10.1016/j.proeng.2012.09.551.